RIKEN BSI BSIS Technical report No02-011

Examples of applications of information-geometric measure to neural data

Hiroyuki Nakahara*†, Shun-ichi Amari*, Masami Tatsuno*

Siu Kang+, Kei Kobayashi‡

* Lab. for Mathematical Neuroscience, RIKEN Brain Science Institute

Wako, Saitama, 351-0198, Japan

+ Dept of Eng., Tamagawa U., Japan

‡ Dept of Math. Eng., U. Tokyo, Japan

† Corresponding author: hiro@brain.riken.go.jp

July 16, 2002

Abstract

This document summarizes the examples that illuminate the merits and applicability of the method proposed in (Nakahara and Amari, accepted), using artificially simulated data as well as experimental data from the prefrontal and dorsal extrastriate visual cortices of monkeys (Anderson et al., 1999). Some examples are the same as in (Nakahara and Amari, accepted), while new examples, particularly including experimental data and the case of auto-correlation,

are included. Thus, this document should be read as a companion of (Nakahara and Amari, accepted).

1 Examples

Here, we show our method using artificial and experimental data. The experimental data is from multi-unit recording data collected simultaneously from the prefrontal and dorsal extrastriate visual cortices of monkeys (Anderson et al., 1999).

1.1 Example 1: Firing of two neurons

We first demonstrate our approach in the case of two neurons, using the artificial spike data in Figs 1-3 and the experimental data in Fig 4.

1.1.1 Coincident firing

In this simulation, we aim to demonstrate a relation between correlation coefficient (COR) and θ, and hypothesis testing under different null hypotheses. Figure 1 A & B gives the mean firing frequency of two neurons and their correlation coefficients (COR; the N-JPSTH), respectively (see the legend for spike generation). The period (a) is assumed as the 'control' period. The neural firing in the control period presumably indicates the resting level activity, which was set to have a very weak correlation here. The firing is almost independent in both periods (b) and (c), whereas it is not independent in the period (d), whose COR is larger than that of the period (a).

Figure 1 C shows θ_3, a quantity in our measure to indicate the pairwise interaction. At first glance, the time-course of θ_3 may look similar to the COR. By a careful inspection, however, they are different (e.g., the relative magnitudes between the pe-

riod (a) and (c) are different for COR and θ). This is simply because $(\eta_1, \eta_2, \theta_3)$ and $(\eta_1, \eta_2, \mathrm{COR})$ form different coordinate systems, although both θ_3 and COR represent the correlational component.

The coordinate system $(\eta_1, \eta_2, \theta_3)$ is dually orthogonal so that we can utilize this property. The Kullback-Leibler (KL) divergence is used to measure discrepancy between two probability distributions, one distribution to be examined and the other to be of the null hypothesis. Using the orthogonality of θ_3 with (η_1, η_2), we can decompose the KL divergence into two terms, one representing the discrepancy in the correlational component and the other the discrepancy in the mean firing. We call the former 'the KL divergence in correlation' below for convenience.

We first examine the KL divergence in correlation against the null hypothesis of independent firing (i.e. $\theta_3 = 0$), which is the probability distribution with the same marginals of the examined probability but with the independent firing. This KL divergence, denoted by KL1, is indicated by the solid line in Fig 1 D. Compared with θ_3, the KL1 takes into account the metric in the probability space. The overall time-course of the KL1 becomes similar to the COR. This is because the plane defined by $\theta_3 = 0$ is the same as the plane defined by COR $= 0$. In Fig 1 D, we also indicate by the dashed line the corresponding p-value, derived from the $\chi^2(1)$ distribution. If the p-value reaches 0.95 in Fig 1 D, for example, it is significant with $p < 0.05$. We observe that the period (d) is significant in Fig 1 D.

We now turn to examine the KL divergence in correlation against the null hypothesis of the averaged activity (including both averaged mean firing rates and averaged coincident firing) in the control period. In Fig 1 E, this KL divergence in correlation, denoted by KL2(1), is indicated by the solid line, while the corresponding p-value, derived from $\chi^2(1)$, is indicated by the dashed line. In Fig 1 E, the period (d) becomes

no longer significant under this null hypothesis. The period (c) is now clearly significant, whereas the period (b) is barely significant, although θ_3 is the same between the two periods (Fig 1 C). This is because the mean firing rates are different between the periods (b, c) and the Fisher information metric takes the geometrical structure into account, not only the degree of the coincident firing (θ_3) but also the marginal probability (i.e. the mean firing rates).

A comparison between Figs 1 D & E illustrates a simple fact that what should be considered as a significant event depends on what is taken as the null hypothesis. In Fig 1 E, where the p-value is from $\chi^2(1)$ formulation, the underlying assumption is that the averaged activity in control period, which is estimated from data in practice, is regarded as a true average activity in control period (see (Nakahara and Amari, accepted) for details). When we are interested in comparing significances between two null hypotheses of independent firing and of the averaged activity in control period, we suggest that the comparison of p-values from $\chi^2(1)$ is informative, as in Fig 1 D & E.

In contrast, since we estimate the average activity in control period from data in practice, a more proper and more conservative hypothesis testing under the null hypothesis of averaged activity in control period is to use a different formulation of likelihood ratio test. This results in using the p-value associated with $\chi^2(2)$ (see (Nakahara and Amari, accepted) for details). In Fig 1 F, we indicate by the solid line the KL2 (2), the KL divergence in the correlation that corresponds to this $\chi^2(2)$ formulation. The dashed line indicates the p-value, now from $\chi^2(2)$. We can observe that the p-value in Fig 1 F gives a more conservative estimate, compared with the p-value in Fig 1 E.

Here, we simply remark that the values of the η-coordinates are provided for all

examples using artificial data. The η-coordinates can be easily converted to the P-coordinates that is used to generate sampled data, by which we estimated θ-coordinates in figures, and given the P-coordinates, it is simple to compute true θ values. In all examples of artificial data, the estimated θ values reasonably match with the true ones (e.g. Fig 8 C).

1.1.2 Mutual information between firing and behavior

Figure 2 shows the decomposition of mutual information (MI) between firing and behavior, using artificial data. We assumed only two choices for the behavior, denoted by s1 and s2. Figure 2 A & B shows the mean firing frequency with respect to s1 and s2, respectively. The mean firing of both neurons is the same between s1 and s2 in the period (a), which was assumed as the 'control' period. In the periods (b, c), assumed as 'test' periods, for simplicity, we have set the mean firing of the two neurons as somewhat 'mirror image' between s1 and s2. The mean firing of each neuron stays the same in the test periods. Notably, however, the mean coincident firing increases in the period (c) only when s2 is given (the period (c) in Fig 2 B).

In Fig 2 C, we show the (total) MI between firing and behavior and its decomposition. The total MI (the solid line in Fig 2 C) exists in the periods (b, c). Its magnitude is larger in the period (c) than in the period (b), although the mean firing of each neuron stays the same in both periods. This is because the coincident firing is modulated by the behavioral choices only in the period (c). This observation can be directly examined by looking into the decomposed MIs (see the figure legend). In brief, we observe that the increase in the total MI in the period (c) comes almost exclusively from the part of the MI by the modulation of the coincident firing (indicated by the dashed dot line in Fig 2 C).

1.1.3 Auto-correlation and cross-correlation

Figures 1 & 2 illustrated applications of the information-geometric measure to the neural firing, which changes over time. The same method can be applied to examine the auto-correlation and the cross-correlation of the neural firing (Toyama et al., 1981a; Toyama et al., 1981b; Eckhorn et al., 1988; Gray et al., 1989; Engel et al., 1991; Ghose and Freeman, 1992; Villa and Fuster, 1992; Nelson et al., 1992; Nicolelis et al., 1995; Kreiter and Singer, 1996; Nowak et al., 1999; Castelo-Branco et al., 2000; Donoghue et al., 1998). We demonstrate the method with the auto-correlation here, while we only note that it can be done similarly with the cross-correlation. In examining the auto-correlation (and/or cross-correlation), one important issue is which of the peaks and/or valleys are significant (Aertsen and Gerstein, 1985; Brody, 1999b; Brody, 1999a; Bar-Gad et al., 2001). The information-geometric measure is relevant in this issue, since it can take into account any non-zero correlated level as the null hypothesis.

In Fig 3 A, the mean firing of a single neuron is plotted over time in both control period (from 0 to 300 ms) and test period (300 - 600 ms). In Fig 3 B, auto-correlations in the former and the latter periods were given by bashed and solid lines, respectively. In Fig 3 B, we observe different peaks and valleys between the two periods. Our question is what peaks and volleys in the test (latter) period are significant, compared with the control (former) period. This can be done similarly to the example in Fig 1. We provided the corresponding θ_3 in Fig 3 C. Using these values and correspondings η_1, η_2 (not shown), we can compute the χ^2 test and in Fig 3 D, we show the p-values of $\chi^2(2)$ test. We simply note that not all but only some peaks (and valleys) become significant ($p < 0.05$). Finally we note that any other null hypothesis, for example, that of independent firing and also previously proposed techniques, e.g., several types of shuffling procedures in auto-correlation (as in Fig 3 B), can be also reformulated in

our method, although not shown here.

1.1.4 Experimental data

Figure 4 shows an example of an application of our method to two neurons experimentally recorded from the prefrontal cortex (Anderson et al., 1999) (see the legend for the task description). The mean firings over all trials and with respect to stimulus in sample period are shown in Fig 4 A & B, respectively. The coincident firing just reaches the significance level after the target goes on ('ton') (Fig 4 C), where it is measured by $p-$value (in $\chi^2(2)$) against the null hypothesis of the averaged activity in the control period. After the target on, that is, appearance of four stimuli, a monkey has to make a saccade towards the stimuli appeared in the sample period in a trial. Hence, the significant coincident firing after 'ton' possibly reflects both the stimulus-selection-related activity and the saccade-related activity.

In Fig 4 D, the MI between firing and behavior (stimulus in the sample period) is indicated by the thick solid line. We note that the MI has the peak after the sample on but is not large after the target on. In other words, while the coincident firing reaches statistical significant level after the target on, it carries no, or a little if any, information of the sample stimulus. Furthermore, in Fig 4 D, the (total) MI is decomposed into the two information, one conveyed by the mean firing rate modulation (indicated by the solid line, which stays nearly the same as the total MI in the figure) and the other conveyed by the coincident firing modulation (indicated by the dotted line). We observe that the total MI is almost the same as the former MI, while the latter MI is nearly zero during a whole trial.

To be sure, we remark that the two neurons shown as an example here are purely chosen for illustrative purpose, so we do not consider the example as indicative of any

typical interaction in the prefrontal cortex.

1.2 Example 2: Firing of three neurons

Here, we demonstrate the case of three neurons, first using artificial data in Figs 5, 6 and then experimental data in Fig 7.

1.2.1 Inspection of triplewise interaction

Figure 5 A gives $\boldsymbol{\eta} = (\boldsymbol{\eta}_1, \boldsymbol{\eta}_2, \boldsymbol{\eta}_3)$, where the firing is assumed as homogeneous for simplicity. The period (a) is assumed as the control period. Figure 5 B shows COR. The COR in the control period is almost zero, while the CORs in the periods (b c) are almost the same as each other, both being different from zero. Yet, when we are more careful in looking into the interaction, using θ_{ij} (Fig. 5 C) and θ_{123} (Fig. 5 D), we can find that the nature of the interaction is largely different between the periods (b) and (c).

The triplewise interaction, θ_{123}, shown in Fig. 5 D, is nearly zero in the periods (a, b). Hence, θ_{ij} in Fig. 5 C indicates the purely pairwise correlation in these periods. On the other hand, since θ_{123} is not zero in the period (c), θ_{ij} in this period does not represent the purely pairwise correlation any more, although it is still correct to say that the pairwise correlation is different between the periods (b, c) by simply observing that θ_{ij}s are different in the two periods. The fact that θ_{123} is not zero in the period (c) indicates that the purely triplewise interaction exists in this period (c), where θ_{123} is negative so that the triplewise interaction is negative.

We can make the above observations more quantitative. In Fig. 5 E, the p-value, derived from $\chi^2(2)$, is to measure the triplewise interaction against the null hypothesis of the activity in the control period. Here we used the decomposition of k-cut = 2

that separate the triplewise interaction from other orders, which take the mean firing rates and the pairwise interaction together (see (Nakahara and Amari, accepted) for details). We observe that the triplewise coincident firing becomes significant only in the period (c).

Figure 5 F indicates the p-value from $\chi^2(8)$, which is to measure the triplewise and pairwise interaction together. Here we used the decomposition of k-cut $= 1$ that separate the mean firing rates (1st-order) from other orders, which take the pairwise and triplewise interactions together (see (Nakahara and Amari, accepted) for details). We can see that both periods (b, c) now become significant.

1.2.2 Mutual information between behavior and firing

Figure 6 shows the decomposition of the MI between firing and behavior, using artificial data. In each of two stimulus conditions, denoted by s1 and s2, the neuron firing is assumed to be homogeneous for simplicity. Figure 6 A & B shows the mean frequency of single neuron firing, of pairwise firing, and of triplewise firing with respect to s1 and s2, respectively. The period (a) was assumed as the 'control' period, while the periods (b-d) were assumed as 'test' periods. For s2, the mean frequency is the same over all periods. For s1, compared with the period (a), only the mean frequency of single neuron firing is different in the period (b); only the mean frequency of pairwise firing is different in the period (c); only the mean frequency of triplewise firing is different in the period (d).

The total MI is shown by the solid line in Figs 6 C & D, while the decomposed MIs by $k-$cut$= 2$ and $= 1$ are shown in Figs 6 C & D, respectively. In the period (b), Fig 6 D indicates that most of behavioral information is carried by modulation of single neuron firing (dashed line in the figure), although some information is also

carried by modulation of the other orders together (dotted line) (see the legend). By inspection of the period (b) in Fig 6 C, we can further observe that the behavioral information is mostly carried by modulation of taking single neuron firing and pairwise firing together (dashed line, which is almost the same as solid line, i.e. the total MI) but is not really carried by triplewise firing (dotted line).

We can inspect the periods (c, d) in a similar manner. In brief, Figs 6 C & D together indicate that most behavioral information is carried by modulation of taking pairwise and triplewise firing together in the period (c) and is carried by modulation of triplewise firing in the period (d).

1.2.3 Experimental data

Figure 7 shows an example, using three neurons of real experimental data recorded from the prefrontal cortex (Anderson et al., 1999). To detect a significant triplewise coincident firing, three p-values are shown in Fig. 7 C. One is against the null hypothesis of independent firing, derived from $\chi^2(1)$ distribution, indicated by dotted line. It indicates the significant coincident firing in the delay period (from soff to ton in the figure) under this null hypothesis. The other two p-values against the null hypothesis of the averaged activity in the control period, one from $\chi^2(1)$ and the other from $\chi^2(2)$ (see (Nakahara and Amari, accepted) for details), are indicated by solid and dashed lines, respectively. Under this null hypothesis, the significant triplewise coincident firing occurs after the target on ('ton'), when measured by the p-value from $\chi^2(1)$. Thus, when we compare the two different null hypotheses, we conclude that the observed significant coincident firing is completely different. When measured by the one from $\chi^2(2)$, which gives a more conservative test, the firing, detected as significant by $\chi^2(1)$ under the latter null hypothesis, becomes not significant. Rigorously speaking, then,

we may say that there is no triplewise significant firing under the latter null hypothesis.

Interestingly, the total MI between firing and behavior (a stimulus in the sample period) in Fig 7 D also has the peak after the target on. This suggests that the significant coincident firing in Fig 7 C may carry information of sample stimulus. However, when we look into the decomposed MIs, which is by $k-$cut$= 2$, we find not much MI conveyed by triplewise firing modulation (indicated by the dotted line in Fig 7 D).

We may note that in Fig 7 D, there is already some amount of MI before sample stimulus appears ('son'). This may look very strange, however, this is an epiphenomena due to a well-known fact that MI can be *overestimated* without correction procedure (Optican et al., 1991; Kjaer et al., 1994; Treves and Panzeri, 1995; Golomb et al., 1997; Panzeri and Treves, 1996). Here we did not use any correction procedure. Still, our above observation that not much MI is conveyed by triplewise firing modulation holds because the estimated MI upper-bounds the true MI.

1.3 Example 3: Interesting set of neuron firing

Here, we demonstrate our method to find an interesting set of neuron firing, using artificial data, and also try to illustrate some practical issues in experimental data analysis. There are two starting assumptions for this demonstration. First, the number of simultaneously recorded neurons is assumed as 10. Second, the number of trials is assumed as 1200 here. The number of trials is severe limitation in real data to detect higher-order interaction and we consider 1200 as conceivable, or not impossible at least.

We follow the procedure under the assumption of full homogeneous firing (Nakahara and Amari, accepted) and ask a question of whether any significant order of firing exists

against the null hypothesis of 'independent' firing at the questioned order. Note that it will be very difficult to investigate our (artificial) data 'faithfully', because the assumed number of trials is 1200 and the dimension of 10 neurons is $2^{10} - 1 = 1023$. The full homogeneous assumption makes computation simpler and helps reduce the dimension of n neuron firing from $(2^n - 1)$ to n dimension so that it circumvents under-sampling problem.

In the procedure, when we find the k-th coincident firing of k neurons insignificant, we go down to the next lower order, i.e., $(k-1)$-th order, ignoring the higher order interaction. In this step, the P-coordinates of $(k-1)$ neurons are easily computed from the P-coordinates of k neurons by

$$P_l^{(k-1)} = P_l^{(k)} + P_{l+1}^{(k)} \quad (l = 0, ..., k), \tag{1}$$

where $P_l^{(k)}$ denotes the probability of the l-tuple firing among k neurons. Let us denote similarly by $\theta_l^{(k)}$ etc. Then, our procedure is to compute $\theta_k^{(k)}$ given $\{P_l^{(k)}\}$ and test it against the null hypothesis of $\theta_k^{(k)} = 0$ by converting its value to p-value in $\chi^2(1)$ distribution.

We specified probability distributions over three periods of a trial to generate spike data (see the figure legend) and call them 'seed probabilities' below for convenience. Given generated sampled data, we employed the procedure. Figure 8 A indicates the estimated mean firing frequency of a single neuron (i.e., the 1st-order mean firing frequency), while Fig 8 B indicates the estimated mean firing frequencies from the 2nd to the 5th-order, which appear from top to bottom in the figure. The period (a) is assumed as control period, in which specified probabilities are independent firing. While the 1st-order mean firing frequency is the same in the periods (b, c) as in the period (a), the mean firing frequencies in higher order (Fig 8 B) are somewhat different but, we may say, do not look so different in the figure. We will see, however,

its intrinsic probabilistic structure significantly different below.

We computed p-value in $\chi^2(1)$ distribution from the seed probabilities and hence, they are exact values which we hope to observe in our estimation. Some of them, only relevant ones, are shown in Fig 8 C. No significant order exists in period (a), simply because the firing in period (a) is independent. In period (b), the p-value of the 4th-order firing exceeds the 0.95 significance level. In period (c), while the p-value of the 4th-order drops far below, the p-value of the 10th-order exceeds the significance level and the p-value of the 7th-order stays around the significance level.

In Fig 8 D, we show corresponding p-values estimated from the sample data, only for 4th and 7th orders. The indicated significant periods in both orders (Fig 8 D) overall follow the exact values (Fig 8 C). Although the 10th-order firing should be significant (as in Fig 8 C), theoretically at least, in our sampled data, it could not be observed. This is due to a sampling problem. Indeed, all of the 8th, 9th, and 10th order firings could not be observed in our sampled data (i.e. $\hat{P}_8^{(10)} = \hat{P}_9^{(10)} = \hat{P}_{10}^{(10)} = 0$) and we started our procedure from the 7th order in the sampled data. This kind of situation will be most likely encountered in real data analysis and relates to the sampling problem even under the full homogeneous assumption, while it also indicates that the significant coincident firing, even if it exists, may not be detected due to the sampling problem. Finally, as a reference, we mention that the other orders do not reach the significant level by both exact and estimated values (results not shown).

2 Conclusion

Examples clearly indicated a number of merits of the method proposed in (Nakahara and Amari, accepted) and also the applicability of the method to real experimental

data.

Acknowledgments

HN is grateful to T. Poggio, Y. Kubuta, R. Gütig, and I. Kitori for their comments. Authors are grateful to K. Anderson, E. Miller for their permission of using their experimental data in this technical report. HN is supported by Grants-in-Aid for Scientific Research on Priority Areas (C) of Ministry of Education, Culture, Sports, Science and Technology (MEXT), Japan.

References

A. M. Aertsen and G. L. Gerstein. 1985. Evaluation of neuronal connectivity: sensitivity of cross-correlation. *Brain Research*, 340(2):341–54.

K.C. Anderson, Asaad W. F., J. D. Wallis, and E.K. Miller. 1999. Simultaneous recordings from monkey prefrontal (PF) and posterior parietal (PP) cortices during visual search. *Society for Neuroscience Abstracts*, 25:355.9.

I. Bar-Gad, Y. Ritov, and H. Bergman. 2001. The neuronal refractory period causes a short-term peak in the autocorrelation function. *Journal of Neuroscience Methods*, 104:155–163.

C. D. Brody. 1999a. Correlations without synchrony. *Neural Computation*, 11(7):1537–1551.

C. D. Brody. 1999b. Disambiguating different covariation types. *Neural Computation*, 11(7):1527–1535.

M. Castelo-Branco, R. Goebel, S. Neuenschwander, and W. Singer. 2000. Neural synchrony correlates with surface segregation rules. *Nature*, 405(6787):685–689.

J. P. Donoghue, J. N. Sanes, N. G. Hatsopoulos, and G. Gaál. 1998. Neural discharge and local field potential oscillations in primate motor cortex during voluntary movements. *Journal of Neurophysiology.*, 79:159–173.

R. Eckhorn, R. Bauer, W. Jordan, M. Brosch, W. Kruse, W. Munk, and H. J. Reitboeck. 1988. Coherent oscillations: a mechanism of feature linking in the visual cortex? *Biological cybernetics*, 60:121–130.

A. K. Engel, P. König, A. K. Kreiter, and W. Singer. 1991. Interhemispheric synchronization of oscillatory neuronal responses in cat visual cortex. *Science*, 252:1177–1179.

G. M. Ghose and R. D. Freeman. 1992. Oscillatory discharge in the visual system: does it have a functional role? *Journal of Neurophysiology*, 68(5):1558–1574.

D. Golomb, J. Hertz, S. Panzeri, A. Treves, and B. Richmond. 1997. How well can we estimate the information carried in neuronal responses from limited samples? *Neural Computation*, 9(3):649–65.

C. M. Gray, A. K. König, P. Engel, and W. Singer. 1989. Oscillatory responses in cat visual cortex exhibit inter-columnar synchronization which reflects global stimulus properties. *Nature*, 338:334–337.

T. W. Kjaer, J. A. Hertz, and B. J. Richmond. 1994. Decoding cortical neuronal signals: network models, information estimation, and spatial tuning. *Journal of Computational Neuroscience*, 1:109–139.

A. K. Kreiter and W. Singer. 1996. Stimulus-dependent synchronization of neuronal responses in the visual cortex of the awake macaque monkey. *Journal of Neuroscience*, 16(7):2381–2396.

H. Nakahara and S. Amari. accepted. Information geometric measure for neural spikes. *Neural Computation*.

J. I. Nelson, P. A. Salin, M. H. Munk, M. Arzi, and J. Bullier. 1992. Spatial and temporal coherence in cortico-cortical connections: a cross- correlation study in areas 17 and 18 in the cat. *Visual Neuroscience*, 9(1):21–37.

M. A. L. Nicolelis, L. A. Baccala, R. C. S. Lin, and J. K. Chapin. 1995. Sensorimotor encoding by synchronous neural ensemble activity at multiple levels of somatosensory system. *Science*, 268:1353–1358.

L. G. Nowak, M. H. J. Munk, A. C. James, P. Girard, and J. Bullier. 1999. Cross-correlation study of the temporal interactions between areas V1 and V2 of the macaque monkey. *Journal of Neurophysiology*, 81:1057–1074.

L. M. Optican, T. J. Gawne, B. J. Richmond, and P. J. Joseph. 1991. Unbiased measures of transmitted information and channel capacity from multivariate neuronal data. *Biological Cybernetics*, 65(5):305–10.

S. Panzeri and A. Treves. 1996. Analytical estimates of limited sampling biases in different information measures. *Network*, 7:87–107.

K. Toyama, M. Kimura, and K. Tanaka. 1981a. Cross-correlation analysis of interneuronal connectivity in cat visual cortex. *Journal of Neurophysiology*, 46:191–201.

K. Toyama, M. Kimura, and K. Tanaka. 1981b. Organization of cat visual cortex as investigated by cross-correlation technique. *Journal of Neurophysiology*, 46:202–214.

A. Treves and S. Panzeri. 1995. The upward bias in measures of information derived from limited data samples. *Neural Computation*, 7:399–407.

A. E. P. Villa and J. M. Fuster. 1992. Temporal correlates of information processing during visual short-term memory. *Neuroreport*, 3:113–116.

Figure legends

Figure 1: Example of two-neuron case to detect the significant pairwise correlation, using artificial data. The spikes of two neurons were generated such that whether a spike exists or not in each bin (1 ms bin width is used) was probabilistically determined in each trial (where the number of all trials was 2000), given an assumed probability $(\eta_1, \eta_2, \eta_{12})$ in each period (a)-(d): The period (a) (from 0 ms to 100 ms) is with $(\eta_1, \eta_2, \eta_{12}) = (0.04, 0.04, 0.0031)$; The period (b) (100 ms - 300 ms) is with $(0.04, 0.04, 0.0016)$; The period (c) (300 - 500 ms) is with $(0.12, 0.12, 0.0144)$; The period (d) (500 - 700 ms) is with $(0.12, 0.12, 0.0260)$. To estimate the probabilities from artificially-sampled data, averaged values in each bin were obtained over all trials and its value in each bin was then finally determined by smoothing over several bins (set as 25 ms). (A) Mean firing frequency for two neurons. Because the mean firing frequency of the two neurons was the same, the two lines are superimposed with very little fluctuation. (B) Correlation coefficient (COR, also called the N-JPSTH). (C) θ_3 $(= \theta_{12})$. (D) Kullback-Leibler (KL) divergence in correlation against the null hypothesis of independent firing (see the main text) is indicated by solid line. The corresponding p-value, derived from the $\chi^2(1)$ distribution, is indicated by dashed line. (E) KL divergence in correlation against the null hypothesis of the averaged activity in the control period. The corresponding p-value, derived from $\chi^2(1)$, is indicated by dashed line. (F) Using the formulation that the firing in the control period and in other periods is from the same correlation level (see (Nakahara and Amari, accepted) for details), the p-value, derived from $\chi^2(2)$, is indicated by dashed line, while the sum of corresponding KL divergences is indicated by solid line.

Figure 2: Example of two-neuron case to obtain mutual information (MI) between firing and behavior and its decomposition, using artificial data. The spikes of two

neurons were generated and estimated in a similar manner to Fig 1. The number of stimulus condition is assumed to be two, denoted dy s1 and s2, and the number of trials per stimulus was 500; In the period (a) (from 0 ms to 100 ms), assumed probabilities $(\eta_1, \eta_2, \eta_{12})$ for s1 and s2 were given as $(0.02, 0.02, 0.002)$ and $(0.02, 0.02, 0.002)$, respectively; In the period (b) (100 - 300 ms), $(0.08, 0.02, 0.004)$ and $(0.02, 0.08, 0.004)$; In the period (c) (300 - 500 ms), $(0.08, 0.02, 0.002)$ and $(0.02, 0.08, 0.015)$. (A, B) Mean firing frequency of the two neuron with respect to s1 (A) and s2 (B), respectively. Solid line indicates the mean firing of one neuron, whereas dashed dot line indicates the mean firing of the other neuron. Dashed line indicates the mean firing of the coincident firing. (C) MI. The (total) MI is indicated by solid line and is decomposed into two terms: the MI by the modulation of the mean firing rate (dashed line) and the MI by the modulation of the pairwise correlation (dashed dot line).

Figure 3: Examples for auto-correlation, using artificially simulated data. (A) Mean frequency of one neuron, for which control and test periods were assumed from 0 to 300 ms and from 300 to 600 ms, respectively (see below for data generation). (B) Auto-correlation in the control period (indicated by dashed line) and in the test period (solid line). (C) The corresponding θ_3 is indicated in the control period (dashed line) and in the test period (solid line). (D) The corresponding p-value derived from $\chi^2(2)$ is indicated. In simulation, spikes were generated by an uniform random variable in $[0, 1]$. A spike was given at time t when the value of the variable exceeded a given periodic function $f(t)$ and no spike was given otherwise. The periodic function used was $f(t) = 5\sin(2\pi f_a t/1000)/200 + 0.955$, where $f_a = 12.5$ (Hz), in the control period and $f(t) = 7\sin(2\pi f_a t/1000)/200 + 7\sin(2\pi f_b t/1000)/300 + 7\sin(2\pi f_c t/1000)/600 + 0.965$, where $f_a = 25$, $f_b = 15$, and $f_c = 10$, in the test period. The number of trials was 50 and the bin width was set as 5 (ms) (with overlapped smoothing window = 5

ms) to obtain the estimated probabilities.

Figure 4: Example of two neurons recorded from the prefrontal cortex (Anderson et al., 1999). Experimental task was a delayed matching sample task. Monkeys were instructed by a fixation cue to fixate, from 'foc' (fixation occur). With a certain delay, one of four stimuli was randomly presented from 'son' (sample on) untill 'soff' (sample off), during which the monkeys continued to fixate on the fixation cue. Then the four stimuli appeared, indicated by 'ton' (target on), and the monkeys were required to make a saccade towards the stimulus shown in the sample period (from son to soff). We took the last 500 ms before 'son', which is within the fixation period (foc - son), as the control period. The values of the coordinates for probability distributions and the firing frequency are obtained by using 25 ms bin with a 140 ms smoothing window. (A) Mean firing frequencies over all trials. Solid and dashed dot lines indicate mean firing of each of two neurons, while dashed line indicates the mean coincident firing. (B) Mean firing frequencies with respect to stimulus in sample period were shown, being superimposed, where different line types (solid, dashed etc) indicate different stimulus. (C) Decomposed KL divergence in correlation is indicated by solid line, while the corresponding p-value, derived from $\chi^2(2)$ distribution, is indicated by dashed line. The significance level for $p < 0.05$ (i.e. $p = 0.95$) is also indicated by horizontal line. (D) Mutual information (MI) between firing and behavior and its decomposition, where the MI is with respect to stimulus in the sample period as 'behavioral choice'. Total MI is indicated by solid line. The MI by the modulation of mean firing rates is shown by solid line, which nearly stays the same as the total MI in a whole trial. The MI by the modulation of coincident firing is indicated by dotted line.

Figure 5: Example of three-neuron case to detect the significant triplewise interaction, using artificial data. The spikes of three neurons were generated and estimated in a similar manner to Fig 1. (A) The η-coordinates. Since we treated a homogeneous case here for simplicity, $\boldsymbol{\eta} = (\eta_i, \eta_{ij}, \eta_{ijk})$ is shown from top to bottom, being superimposed with the same order of η-coordinates. (B) Correlation coefficients (COR) of three pairs of neural firing are shown, being superimposed. (C) The second order, $\theta_{ij} = \{\theta_{12}, \theta_{13}, \theta_{23}\}$. (D) The third order, θ_{123}. (E) The p-value, from $\chi^2(2)$, to indicate triplewise coincident firing against the null hypothesis of the average activity in the control period. (F) The p-value from $\chi^2(8)$, to indicate pairwise and triplewise coincident firing together against the null hypothesis of the average activity in the control period. As for spike data generation, the number of trials are set as 2000 and the spike probability (in 1 ms bin) is assumed to be homogeneous in each period; $\boldsymbol{\eta} = (\eta_i, \eta_{ij}, \eta_{ijk}) = (0.0450, 0.00258, 0.00020)$ in period (a), $\boldsymbol{\eta} = (0.0450, 0.0090, 0.0040)$ in period (b), and $\boldsymbol{\eta} = (0.0449, 0.0090, 0.0001)$ in period (c). Arrows in the right hand side in Fig B, C and D indicate true values (see Fig 1 legend).

Figure 6: Example of three-neuron case to obtain mutual information (MI) between firing and behavior and its decomposition, using artificial data. The spikes of three neurons were generated and estimated in a similar manner to Fig 1. (A, B) Mean firing frequency of the three neurons with respect to s1 (A) and s2 (B). In each figure, the mean firings of a single neuron, of the pairwise coincident firing, and of the triplewise coincident firing are indicated from top to bottom. (C) MI and its decomposition by $k-$cut$=$ 2. The total MI is indicated by solid line. The two decomposed MIs, one by modulation of taking the mean firing rate and the pairwise interaction together and the other by modulation of the triplewise interaction, are indicated by dashed

and dotted lines, respectively. (D) MI and its decomposition by $k-$cut$= 1$. The total MI is indicated by solid line. The two decomposed MIs, one by modulation of the mean firing rate and the other by modulation of taking the pairwise and triplewise interactions together, are indicated by dashed and dotted lines, respectively. As for spike data generation, the number of trials per stimulus was 1000 and in each stimulus, the spike probability is assumed to be homogeneous: For s2, assumed probabilities are $(\eta_i, \eta_{ij}, \eta_{ijk}) = (0.08, 0.00704, 0.00041)$ over all the periods (a-d). For s1, assumed probabilities are $(\eta_i, \eta_{ij}, \eta_{ijk}) = (0.08, 0.00704, 0.00041)$ in the period (a). Compared with these probabilities, η_i changed to 0.12 in the period (b), η_{ij} changed to 0.00049 in the period (c), and η_{ijk} changed to 0.00700 in the period (d).

Figure 7: Example of three neurons recorded from the prefrontal cortex in the same task as in Fig 6 (Anderson et al., 1999). (A) Mean firing frequencies over all the four stimulus. Each of three solid lines indicates the mean firing of three neurons. Each of three dashed dot lines indicate the pairwise mean firing. Thick solid line indicates the triplewise mean firing. (B) Mean firing frequencies with respect to stimulus in sample period, being superimposed, where different line types indicate different stimulus. (C) Examination of triplewise coincident firing. Three p-values are shown: one derived from $\chi^2(1)$ distribution (indicated by dotted line) against the null hypothesis of independent firing and, two, derived from $\chi^2(1)$ (solid line) and from $\chi^2(2)$ (dashed line), against the null hypothesis of the averaged activity in the control period. (D) Mutual information (MI) between firing and behavior and its decomposition by k-cut $= 2$. The MI is shown with respect to stimulus in the sample period, as 'behavioral choice'. The total MI is indicated by solid line. The MI by modulation of taking mean firing rates and the pairwise interaction together is also indicated by solid line, which is nearly the same as the total MI. The MI by modulation of triplewise interaction is

indicated by dotted line.

Figure 8: Example of ten-neuron case to find an interesting set of neurons, using artificially simulated data. The spikes of ten neurons were generated and estimated in a similar manner to Fig 1. The number of trials was set as 1200. The spike probabilities are assumed to be homogeneous so that we only define 10 dimensional coordinates, which we indicate here by η-coordinates. In all periods (a-c), η_1 is fixed as 0.010. In period (a), the firing is assumed to be independent, i.e. $\eta_k = \eta_1^k$ $(k = 2, ..., 10)$. In period (b), $\eta_k = 0.0125 \times (0.285)^{k-2}$ $(k = 2, ..., 10)$. In periods (c), $\eta_2 = 0.0125, \eta_3 = 0.0020$, and $\eta_k = 0.0003 \times (0.5)^{k-4}$ $(k = 4, ..., ..., 10)$, to which there are made very small adjustments. (A) Mean firing frequency (of the 1st order). (B) Mean firing frequencies of the 2nd, 3rd, 4th and 5th order, which appears from top to bottom. (C) Theoretically expected p-values in $\chi^2(1)$ for the 4th (indicated by dashed line), 7th (by solid line) and 10th order (by dotted line). (D) Estimated p-values for the 4th (by dashed line) and 7th order (by solid line).

Figure 1

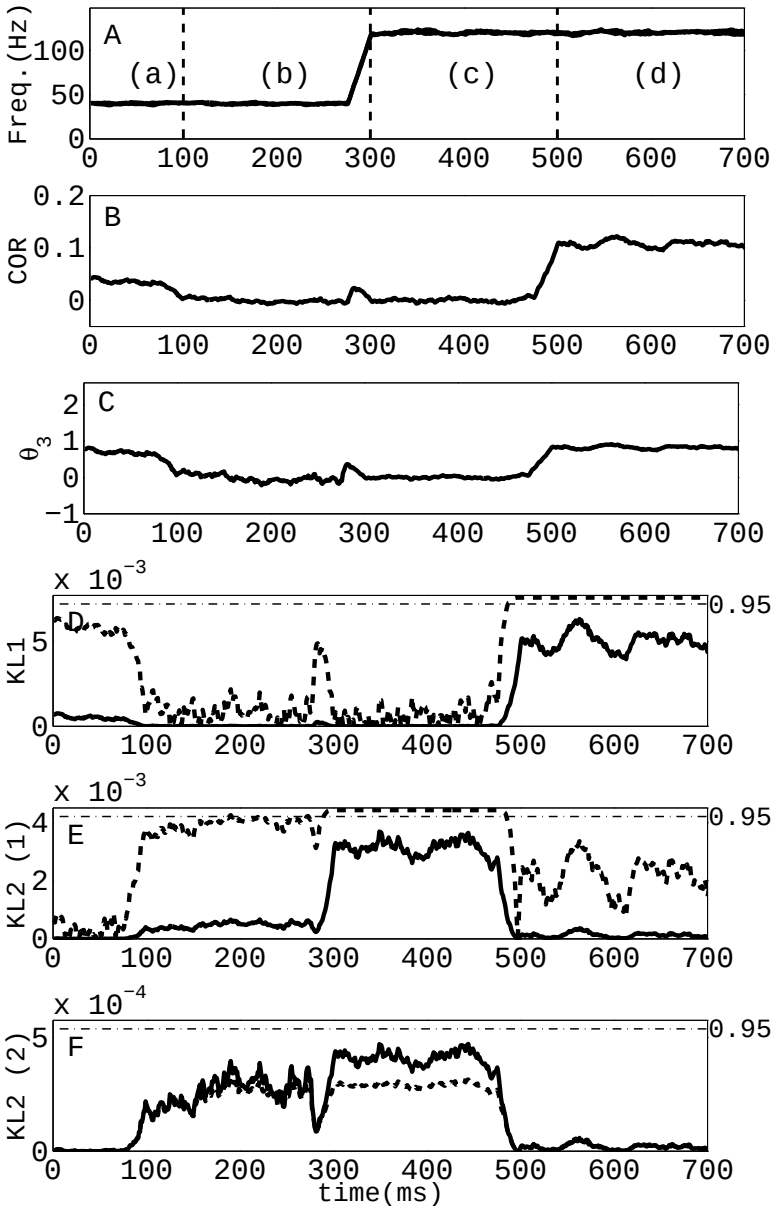

Figure 1/Nakahara

Figure 1:

Figure 2

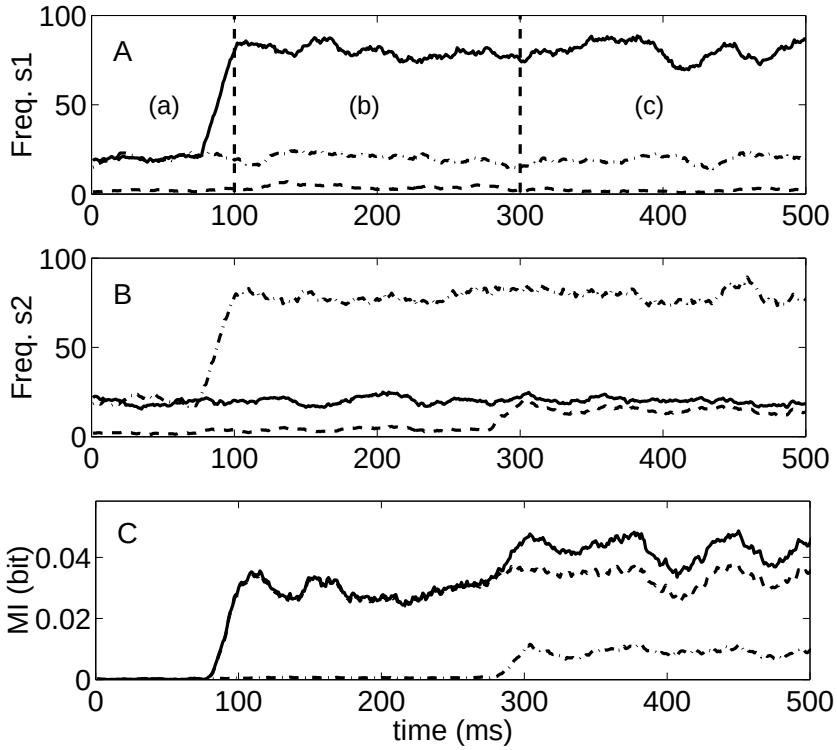

Figure 2/Nakahara

Figure 2:

Figure 3

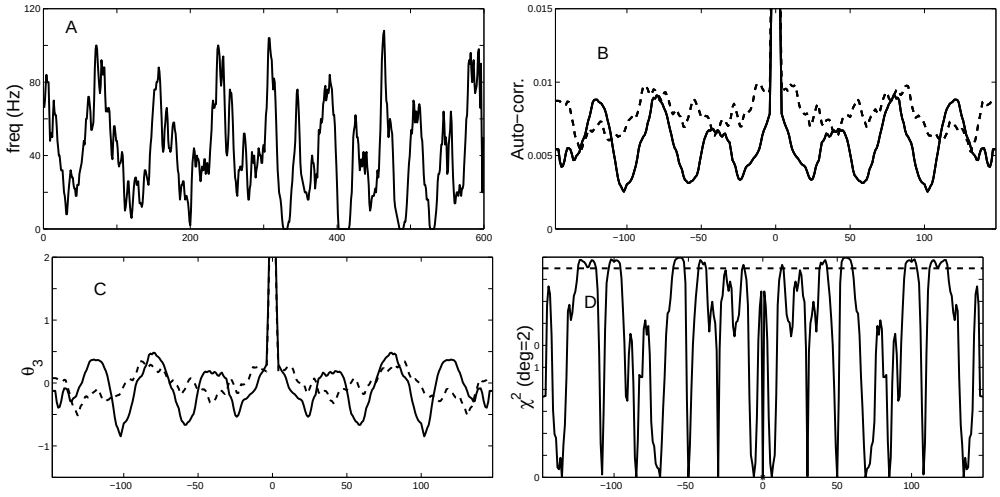

Figure 3/Nakahara

Figure 3:

Figure 4

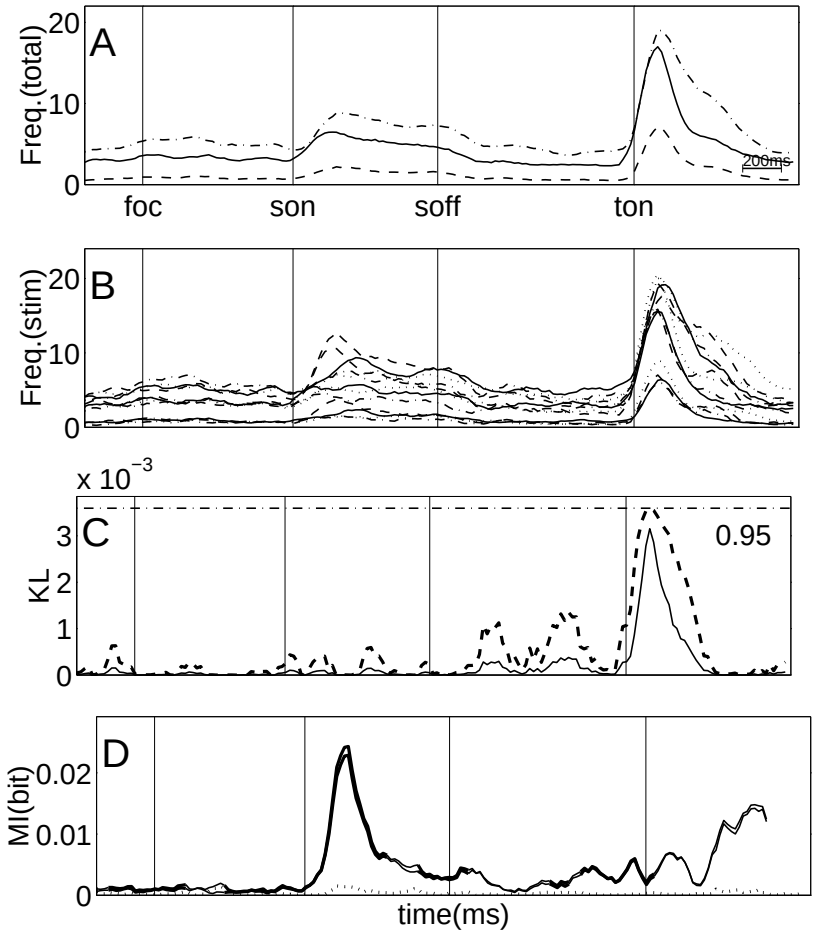

Figure4/Nakahara

Figure 4:

Figure 5

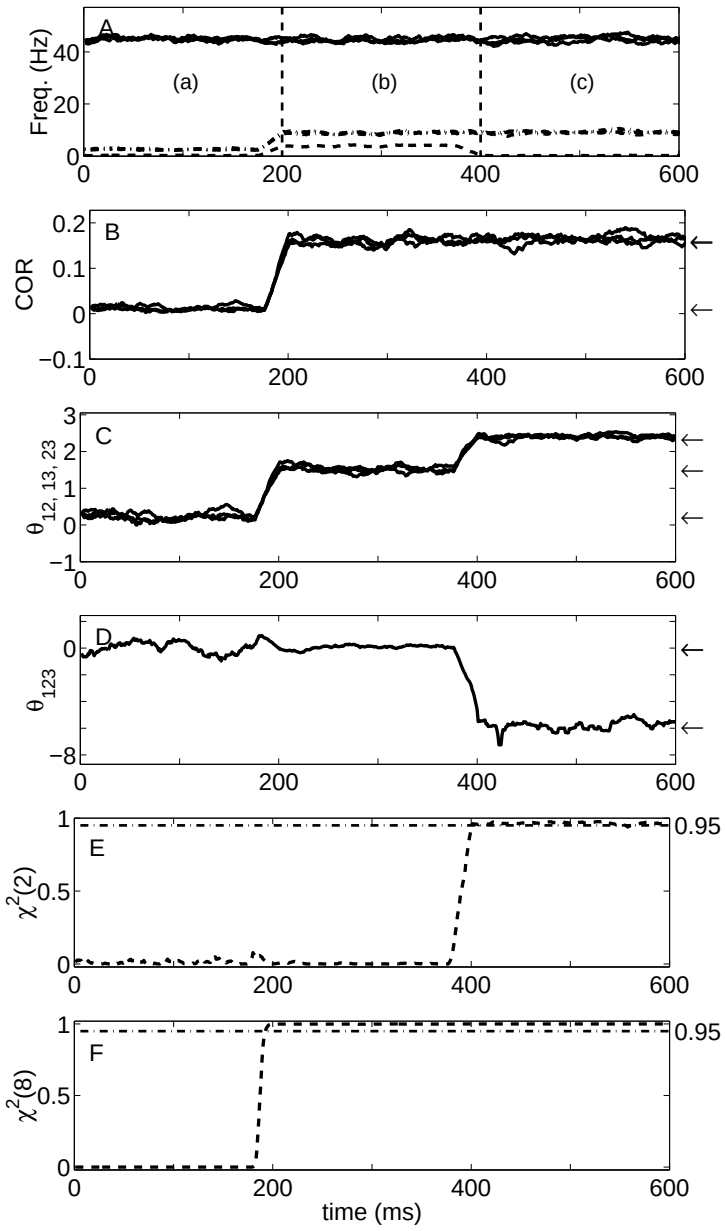

Figure5/Nakahara

Figure 5:

Figure 6

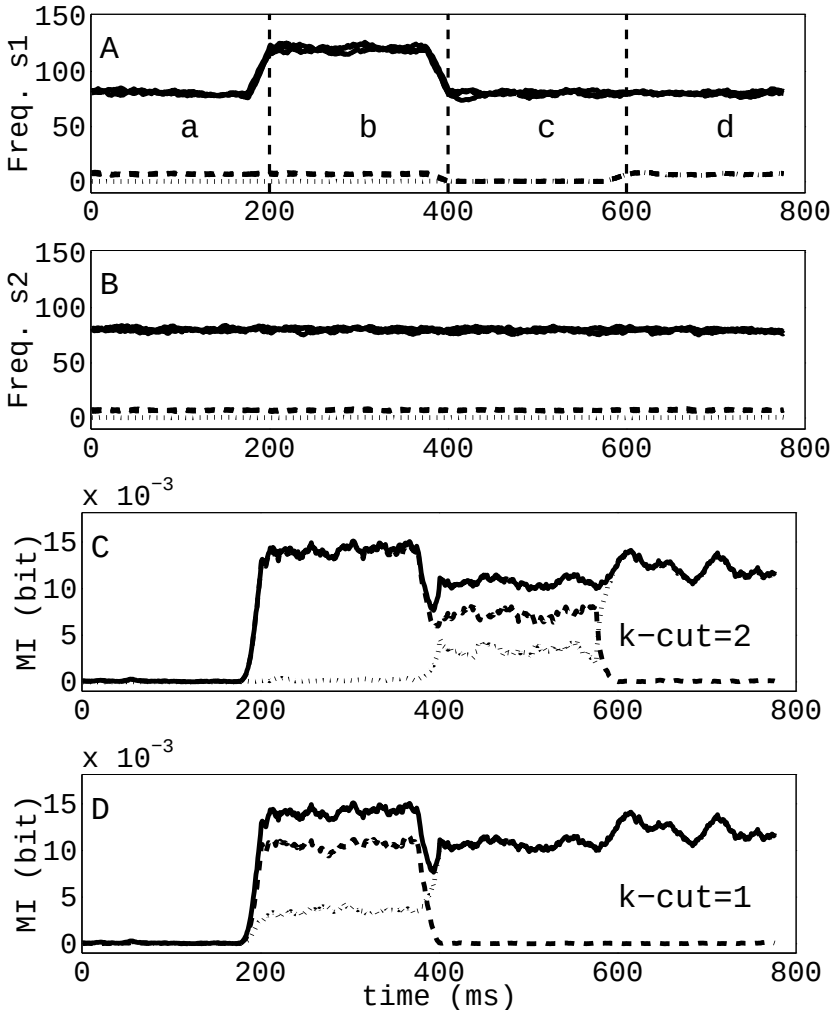

Figure6/Nakahara

Figure 6:

Figure 7

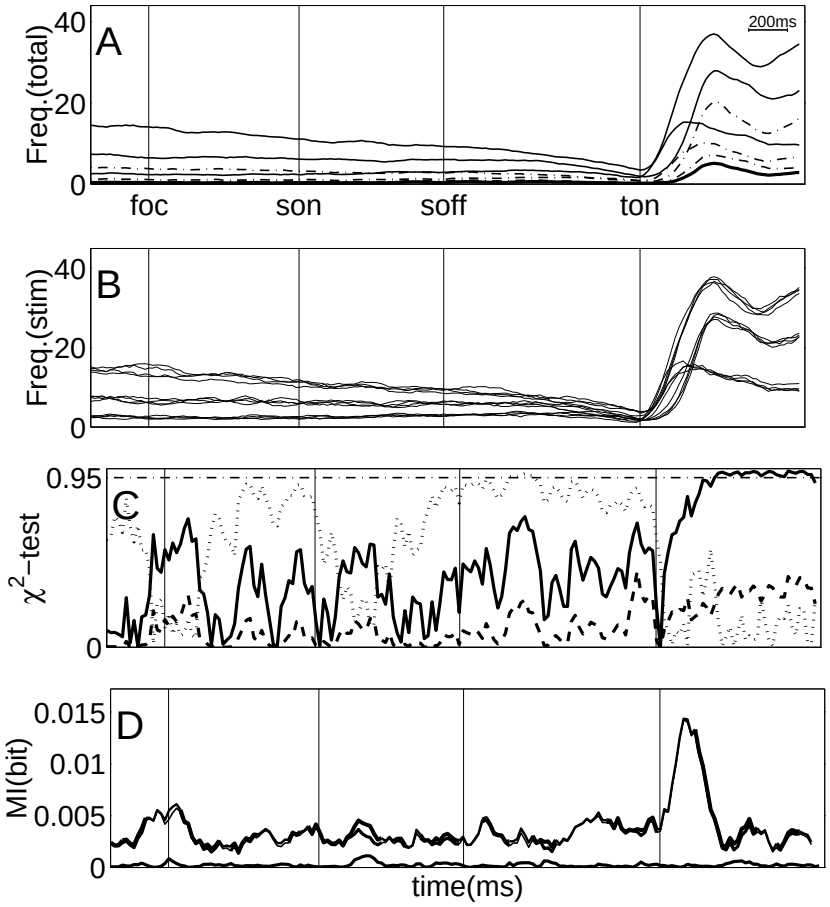

Figure7/Nakahara

Figure 7:

Figure 8

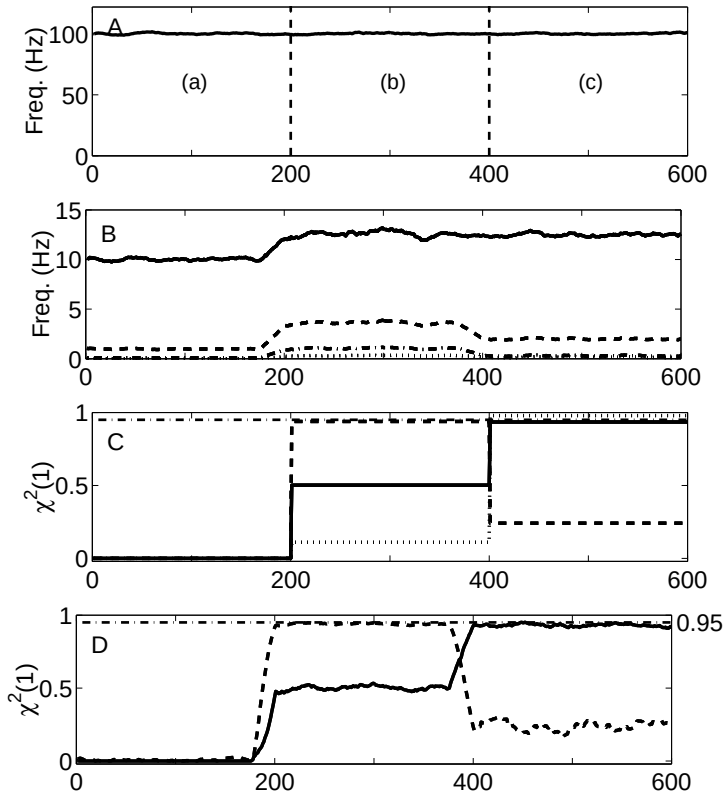

Figure 8/Nakahara

Figure 8: